Supporting Information: Intermolecular Background Decay in RIDME Experiments

Katharina Keller[1], Mian Qi[2], Christoph Gmeiner[1], Irina Ritsch[1], Adelheid Godt[2], Gunnar Jeschke[1], Anton Savitsky[3], Maxim Yulikov[1,*]

1. Detailed author contribution statement

This work consisted of an initial set of RIDME background measurements for Gd(III) and Mn(II) (1st set), the study of RIDME background dependencies on the transverse evolution delay times for metal complexes and spin labeled protein samples, the derivation of the theoretical model, the final set of RIDME background measurements on metal complexes, demonstrating the features of the derived equations (2nd set), and the set of RIDME background measurements on spin labeled protein samples. The 1st set was designed by M.Y. and A.S., the 2nd set was designed by M.Y. and K.K. The RIDME background measurements for the 1st and 2nd set were performed by K.K. The dependency of the RIDME background on transverse evolution delay times was discovered and investigated by K.K. and I.R. The measurements on spin labeled protein samples were performed by K.K. The theoretical description was derived by M.Y. The fitting of the RIDME data was performed by K.K., the error analysis was performed by K.K. and M.Y. The spin-labeled protein sample was prepared by C.G. The synthesis route was designed and the PyMTA complexes of Cu(II), Gd(III) and Mn(II) were synthesized by M.Q. and A.G. The data were discussed and the manuscript was written with contributions from all authors.

*corresponding author: maxim.yulikov@phys.chem.ethz.ch

[1]Laboratory of Physical Chemistry, Department of Chemistry and Applied Biosciences, ETH Zurich, Vladimir-Prelog-Weg 2, 8093 Zurich, Switzerland.

[2]Faculty of Chemistry and Center for Molecular Materials (CM_2), Bielefeld University, Universitätsstraße 25, 33615 Bielefeld, Germany

[3]Physics Department, Technical University Dortmund, Otto-Hahn-Straße 4a, 44227, Dortmund, Germany

2. Synthesis of Cu-PyMTA

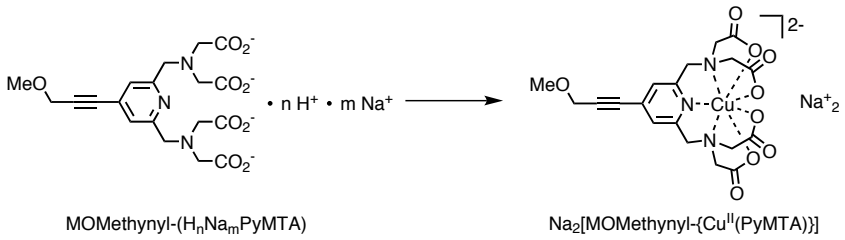

Figure SI 1: Synthesis route of Cu-PyMTA.

Na_2[MOMethynyl-{Cu^{II}(PyMTA)}]. MOMethynyl-(H_nNa_mPyMTA)[1] (2.652 mg, contains 5.45 μmol of the structural motif [(4-MOMethynyl-H_4PyMTA) - 4 H^+]$^{4-}$ as determined by quantitative ^{1}H NMR spectroscopy)[2] was dissolved in D_2O (500 μL). A solution of $CuCl_2$ in D_2O (0.05 M, 103.6 μL, 5.18 μmol), which had a very pale blue colour, was added whereupon the colour of the solution changed to blue. A solution of NaOD in D_2O (0.10 M, 150 μL, 15 μmol) was added to rise the pH of the solution to pH 8.2. The solution was diluted with D_2O (336.8 μL) to obtain a 5 mM solution of Na_2[MOMethynyl-{Cu^{II}(PyMTA)}] in D_2O containing NaCl. Mass-spectroscopy (ESI) shows the corresponding peaks: m/z = 247.8 [M - 2Na]$^{2-}$, 217.3 [(4-MOMethynyl-H_4PyMTA) - 2H]$^{2-}$.

3. Examples of the fitting procedure

RIDME traces were fitted by a stretched exponential function (SE model) of the form $c \cdot \exp(-(kt)^{d/3})$, a sum of two stretched exponential functions (SSE model) of the form $c_a \cdot \exp(-(k_a t)^{d_a/3}) + c_b \cdot \exp(-(k_b t)^{d_b/3})$ or a product of two stretched exponential functions (PSE model) of the form $c \cdot \exp(-(k_a t)^{d_a/3}) \cdot \exp(-(k_b t)^{d_b/3})$ using a nonlinear least-square fitting criterion without prior normalization. The zero time point of the data traces was set to the expected zero time of 120 ns due to the sequence settings used in the RIDME experiment. The start point of the fitting routine was either set to the zero time point or shifted forward, thus cutting out the echo crossing artefact at zero time (see for example Figure SI 2). This allowed for estimating an additional error, introduced by the mentioned artefact as well as the variation of the stretched exponential parameters due to cut of an initial part of the trace. Each such time trace was fitted by applying 20 different,

random starting parameter sets, and the best set of k and d parameters out of these 20 runs was selected. The 95% confidence of this fit (MATLAB function 'nlparci') was used to estimate the error. The best d and k set of parameters was then computed as the average over the results for different starting positions. The resulting error was taken as the largest error between the single-start-time error estimate, and the width of the distribution of the best-fit values over the range of starting positions. If a later starting point resulted in a significantly poorer fit, it was not taken into account for calculating the average value of d as well as k. Similarly, if there was a clear mismatch of the initial region for the fit starting at the zero time point due to a strong echo crossing artefact, those data points were excluded. Figure SI 2 and 3 show two typical examples of such a fitting routine.

If the data trace was not decayed to at least the 1/e value, errors were approximately estimated by manually varying d and adjusting k according to $\left\{(k \cdot t_{\max})^{(d/d_{\mathrm{var}})}/t_{\max}\right\}$, to match the best fit curve at the last time point. This was done because the largest error in fitting such short traces appears due to the correlated change of d and k, which is not catched by the 'nlparci' function. This approach must still have somewhat underestimated the errors for d and k, but it resulted in larger error bars than the gradient-based calculation for short RIDME background decay traces. We assume that these estimates are comparable to the actual error bars in RIDME background fits. The ultimately accurate error estimation would include the analysis of the local Hessian matrices, which would be computationally too expensive for such large sets of data. This is also the reason why such a procedure is not offered in the MATLAB package.

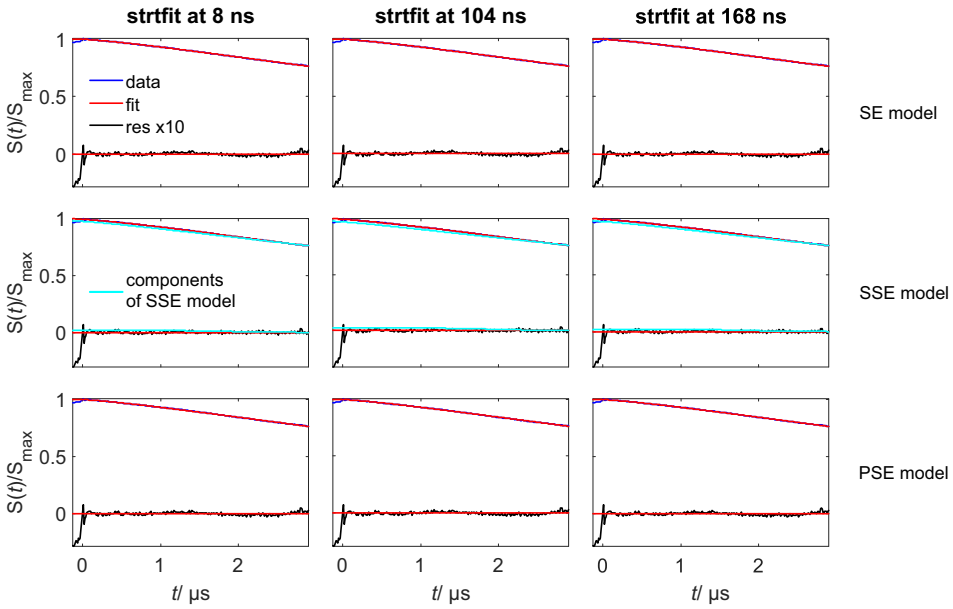

Figure SI 2: RIDME background fits for 100 μM Gd-PyMTA in deuterated matrix at 10 K in W band. $T_{\mathrm{mix}} = 41$ μs, $d_1 = 0.4$ μs, $d_2 = 3.2$ μs. Top: Fit by SE model; Middle: Fit by SSE model; Bottom: Fit by PSE model. From left to right: increasing time of the fitting starting point after zerotime. Note measurement are scaled to maximum intensity excluding the zero-time artefact.

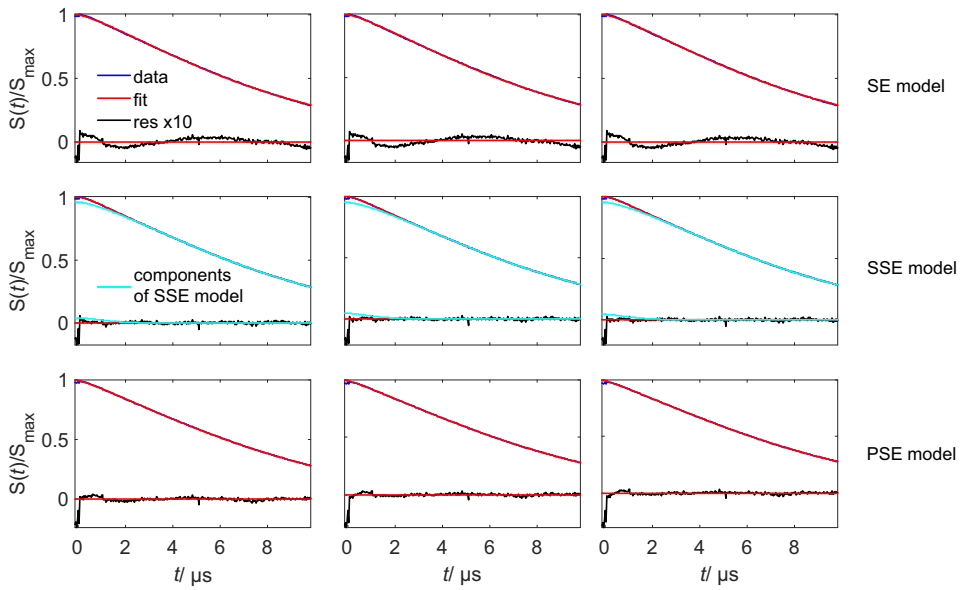

Figure SI 3: RIDME background fits for 100 μM Gd-PyMTA at 10 K in W band. $T_{\mathrm{mix}} = 97$ μs, $d_1 = 10$ μs, $d_2 = 10.2$ μs. Top: Fit by SE model; Middle: Fit by SSE model; Bottom: Fit by PSE model. From left to right: increasing time of the fitting starting point after zerotime.

4. Influence of the detection position in RIDME background decays

Moving the detection position away from the center of the Gd(III) spectrum induces a faster background decay in RIDME measurement of 100 μM Gd-PyMTA.

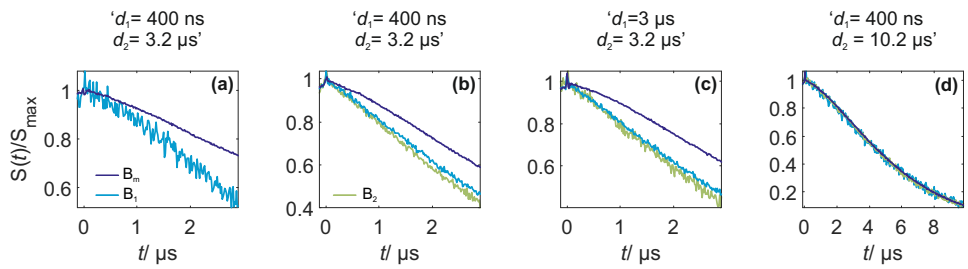

Figure SI 4: Comparison of RIDME background decay of 100 μM Gd-PyMTA in W band at various detection positions. $T_{\mathrm{mix}} = 65$ μs $\approx T_1$; $\mathrm{B_m}$ corresponds to detection at maximum of Gd(III) spectrum (purple lines), $\mathrm{B_1} = \mathrm{B_m} - 150$ G (blue lines), $\mathrm{B_2} = \mathrm{B_m} - 750$ G (green lines), (a) 30 K. (b-d) 10 K. Note measurement are scaled to maximum intensity excluding the zero-time artefact.

It is accompanied by an increase of the characteristic decay rate k and a decrease in the background dimensionality d, thus leading to more mono-exponential functions. The effects diminish at longer dipolar evolution delays $d_2 > T_{\mathrm{m_{outer}}}$, with $T_{\mathrm{m_{outer}}}$ being the transverse relaxation time of the outer Gd(III) transitions.

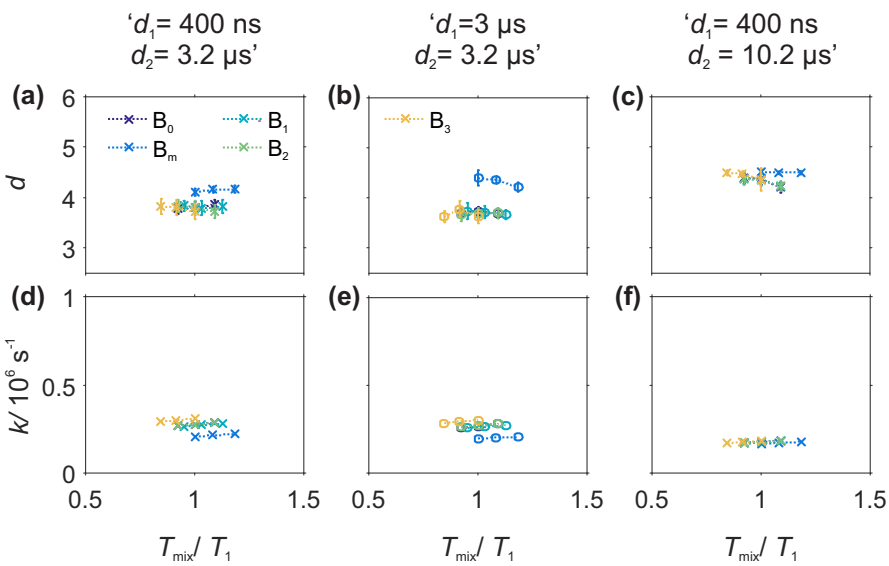

Figure SI 5: Comparison of the stretching exponent d (a-c) and decay rate k (d-f) versus the relative mixing time T_{mix}/T_1 at given pulse sequence settings (left to right) for different detection fields in W band at 10 K for 100 μM Gd-PyMTA in deuterated matrix. (a, d) $d_1 = 0.4$ μs, $d_2 = 3.2$ μs; (b, e) $d_1 = 3$ μs, $d_2 = 3.2$ μs; (c, f) $d_1 = 0.4$ μs, $d_2 = 10.2$ μs. $\mathrm{B_m}$ corresponds to detection at maximum of Gd(III) spectrum (blue lines), $\mathrm{B_0} = \mathrm{B_m} +$ 150 G (purple lines), $\mathrm{B_1} = \mathrm{B_m}$ - 75 G (cyan lines), $\mathrm{B_2} = \mathrm{B_m}$ - 150 G (green lines), $\mathrm{B_3} = \mathrm{B_m}$ - 750 G (yellow lines).

5. Additional Figures to Section 4.3

Figure SI 6 and SI 7 show decay rates k with enlarged axis scales as addition to main Figures 7 and 8, respectively.

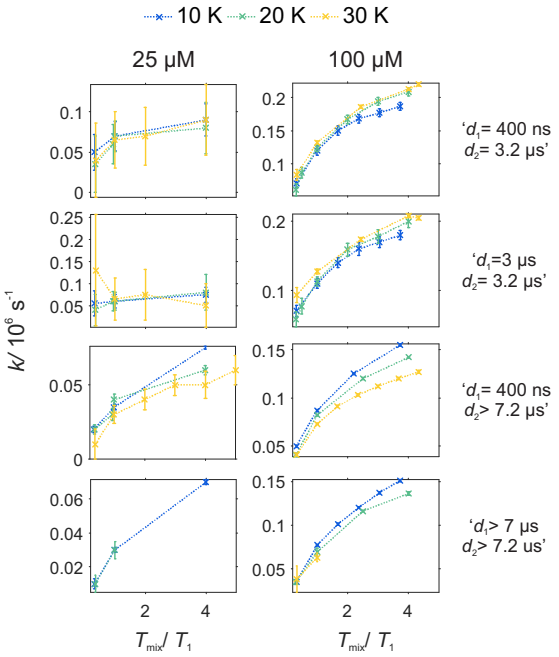

Figure SI 6: Comparison of decay rate constant k versus the relative mixing time T_{mix}/T_1 obtained from the analysis of experimental W-band RIDME decays in deuterated solvent matrix at given pulse sequence settings (top to bottom) and spin concentration (left to right). The measurement temperature is color encoded: blue 10 K, green 20 K, yellow 30 K.

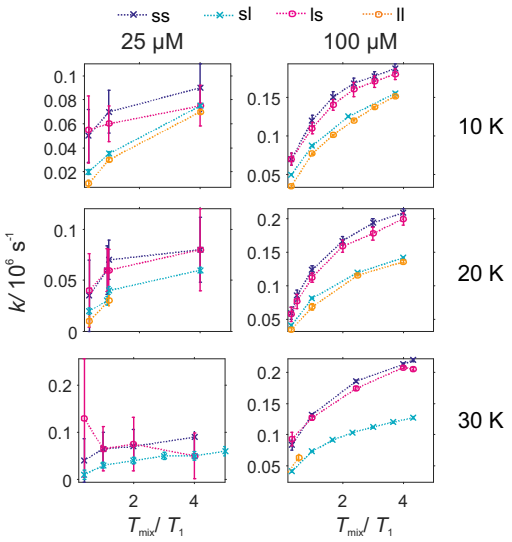

Figure SI 7: Comparison of decay rate constant k versus the relative mixing time T_{mix}/T_1 obtained from the analysis of experimental W-band RIDME decays in deuterated solvent matrix at given measurement temperature (top to bottom) and spin concentration (left to right). The pulse sequence settings are color encoded: purple line (ss): $d_1 = 0.4$ μs, $d_2 = 3.2$ μs; dark blue line (ls): $d_1 = 3$ μs, $d_2 = 3.2$ μs; light blue line (sl): $d_1 = 0.4$ μs, $d_2 = 10.2$ μs and green line (ll): $d_1 = 10$ μs, $d_2 = 10.2$ μs. At 30 K, the long d_2 values was only set to 7.2 μs and correspondingly d_1 to 7 μs. At 20 K the green line (lm) corresponds to $d_1 = 7$ μs, $d_2 = 7.2$ μs and the yellow line (sm) to $d_1 = 0.4$ μs, $d_2 = 7.2$ μs. Cross marks correspond to a short interpulse daly d_1 of 400 ns; circles to a long d_1 on the order of d_2.

6. Background decay in Cu-/Mn-PyMTA complexes

For Cu-PyMTA and Mn-PyMTA similar observations as for Gd-PyMTA were made. The best fits with a single stretched exponential function resulted in stretching exponent values d between 3 and 6. As in case of Gd-PyMTA, the d value was decreasing for longer d_2 values. There is also a slight trend for decreasing d with increasing T_{mix}/T_1.

The decay rate k is increasing with T_{mix}/T_1. As described in the main text for Gd-PyMTA, k is reduced when the temperature, the delay d_2, and/or the delay d_1 are increased.

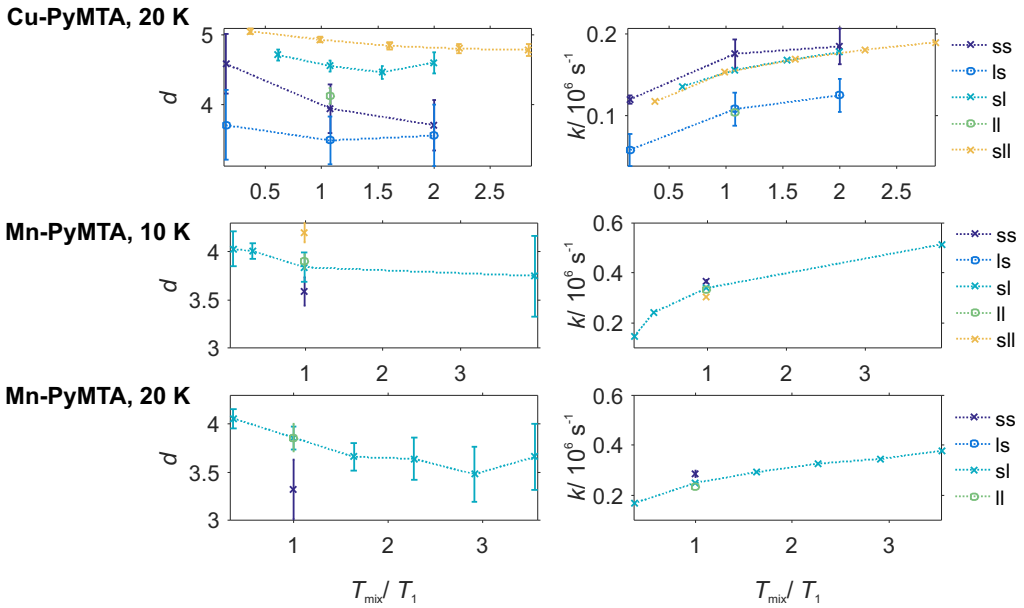

Figure SI 8: Comparison of stretched exponential parameters d (left) and k (right) for Cu(II)- and Mn(II)-PyMTA each of 100 μM spin concentration in deuterated matrix and Q band. The sequence parameters were set as follows:
For Cu(II): short short (ss): $d_1 = 0.4$ μs, $d_2 = 2$ μs, long short (ls): $d_1 = 2$ μs, $d_2 = 2$ μs, short long (sl): $d_1 = 0.4$ μs, $d_2 = 5$ μs, long long (ll): $d_1 = 5$ μs, $d_2 = 5$ μs, short longer (sll) $d_1 = 0.4$ μs, $d_2 = 7$ μs;
For Mn(II): short short (ss): $d_1 = 0.4$ μs, $d_2 = 2.2$ μs, short long (sl): $d_1 = 0.4$ μs, $d_2 = 4.2$ μs, long long (ll): $d_1 = 4$ μs, $d_2 = 4.2$ μs, short longer (sll) $d_1 = 0.4$ μs, $d_2 = 8.2$ μs.

7. Background decay in spin-labeled protein mutant RRM34 Q388C

The differences in the background fitting parameters for deuterated and protonated buffer solutions are shown in Figure SI 9 and SI 10. An increasing proton content leads to an increase in the decay rate k. Further, the decay rate k behaves as observed for the model compounds, with k increasing with increasing mixing time. However, the increase of k is slow and almost linear in the studied mixing time range due to the dominance of the approximately temperature-independent nuclear spin diffusion processes in the studied range. The similarity of the k parameters at different measurement temperatures further supports the assumption of temperature independence of nuclear-spin processes in the studied range.

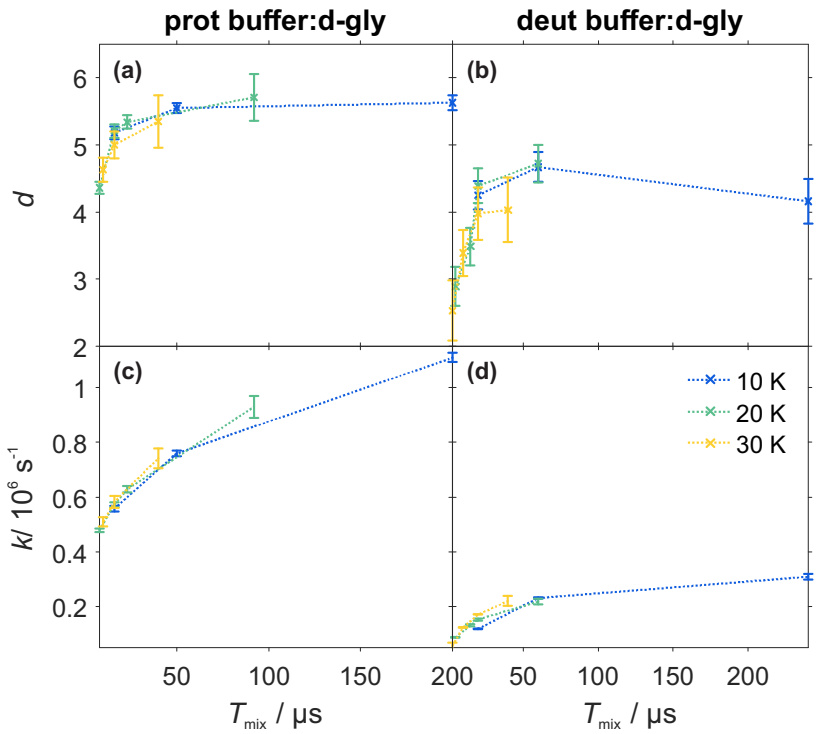

Figure SI 9: Comparison of stretched exponential parameters d and k for RRM34 Q388C Gd(III)-DOTA in W band. (a, c) in H_2O buffer:glycerol-d8 with $d_1 = 0.4$ μs, $d_2 = 4.2$ μs, $T_{1,e} = 50$ μs; (b, d) in D_2O buffer:glycerol-d8 with $d_1 = 0.4$ μs, $d_2 = 10.2$ μs. (a, b) stretched exponent d and (c, d) decay rate k.

The dimensionality d exhibits a more Gaussian-like decay shape for proton-dominated environments. As for the decay rate k, the d parameters are very

similar at different measurement temperatures. The dimensionality d is increasing with increasing d_1 as observed in the metal-PyMTA samples. Contrary to the metal-PyMTA complexes, for the RRM34 sample the stretching exponent d is reduced for longer dipolar evolution times d_2 (see Figure SI 10 (b)). However, it is important to note that traces of long d_2 were in most cases cut to allow for a sufficiently good fit using a single stretched exponential function. Overall fits by a sum of two stretched exponential functions were more suitable in the description of samples in deuterated buffer and long d_2 as shown in Figure SI 10.

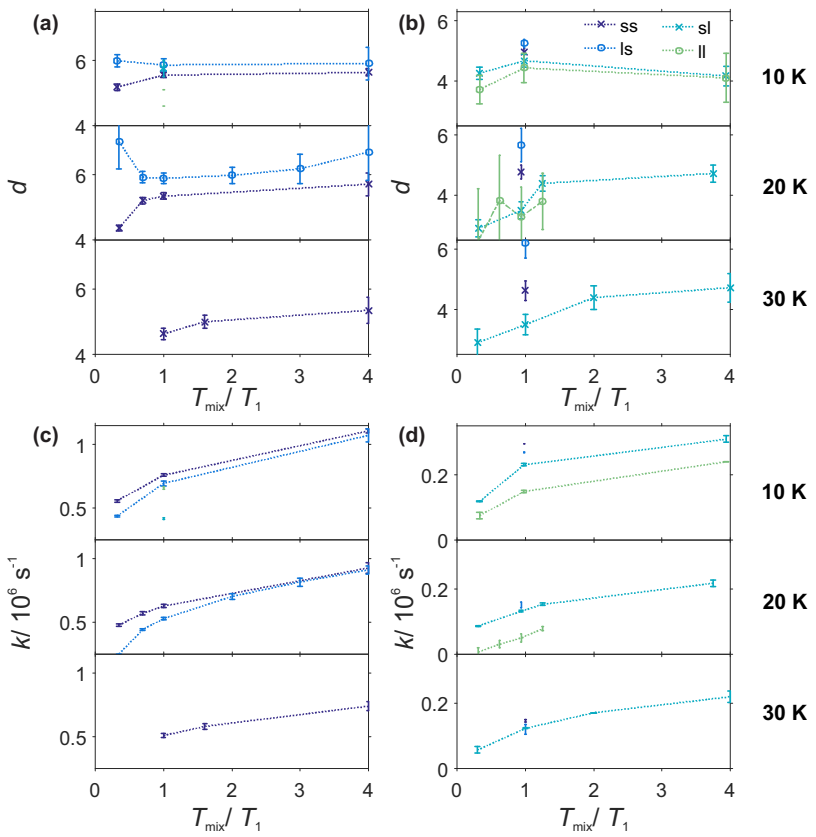

Figure SI 10: Comparison of stretched exponential parameters d and k for RRM34 Q388C Gd(III)-DOTA in W band. (a, c) in H_2O buffer:glycerol-d8, $T_{1(1/e)} = 50$ μs; (b, d) in D_2O buffer:glycerol-d8, $T_{1(1/e)} = 60$ μs. (a, b) stretched exponent d and (c, d) decay rate k. The sequence parameters were set as follows: short short (ss): $d_1 = 0.4$ μs, $d_2 = 4.2$ μs, long short (ls): $d_1 = 4$ μs, $d_2 = 4.2$ μs, short long (sl): $d_1 = 0.4$ μs, $d_2 = 5.2$ (protonated case) or 10.2 μs (deuterated case), long long (ll): $d_1 = 10$ μs, $d_2 = 10.2$ μs. Note that the mixing time is normalized by the electronic relaxation times of Gd(III). The near absence of the changes in d and very weak changes in k for the changes in mixing time on the order of electronic T_1 confirm that the nuclear-driven mechanisms play the major role in these RIDME background shapes.

8. Relation of relaxation times to trace settings

The pulse sequence settings used in the systematic study on Gd-PyMTA at different spin concentration and measurement temperature are given in Table 1.

	short short (ss)	short long (sl)	long short (ls)	long long (ll)
d_1/μs	0.4	0.4	3	10
d_2/μs	3.2	10.2	3.2	10.2
d_1/d_2	8	25.5	1.07	1.02
$(d_1+d_2)/\mu$s	3.6	10.6	6.2	20.2
$(d_2-d_1)/\mu$s	2.8	9.8	0.2	0.2

Table SI 1: Pulse sequence combinations for the systematic study on Gd-PyMTA.

The fitted relaxation times using a SE model, the ratio T_m/T_1 and their relation to the dipolar evolution times d_2 are given in Table 2.

Conc	T/ K	T_m/ μs	T_1/ μs	T_1/T_m	$d_{2,\mathrm{short}}/T_1$	$d_{2,\mathrm{long}}/T_1$
25 μM	10	23.3 ± 0.3	47.5 ± 1.3	2.04	0.07	0.22
	20	11.7 ± 0.1	17.4 ± 0.6	1.48	0.18	0.59
	30	6.2 ± 0.1	8.1 ± 0.3	1.30	0.40	1.26
100 μM	10	22.2 ± 0.2	41.3 ± 0.9	1.86	0.08	0.25
	20	11.7 ± 0.1	15.9 ± 0.3	1.36	0.20	0.64
	30	7.2 ± 0.1	8.7 ± 0.2	1.21	0.37	1.17
500 μM	10	11.2 ± 0.3	45.1 ± 1.8	4.03	0.07	0.23
	20	5.9 ± 0.1	15.3 ± 0.5	2.59	0.21	0.67
	30	4.7 ± 0.1	6.6 ± 0.3	1.40	0.48	1.55

Table SI 2: Relaxation times T_m and T_1 in μs from 10-30 K in W band for Gd-PyMTA at different concentrations (25, 100, 500 μM). $d_{2,\mathrm{short}} = 3.2$ μs; $d_{2,\mathrm{long}} = 10.2$ μs.

References

References

[1] K. Keller, M. Zalibera, M. Qi, V. Koch, J. Wegner, H. Hintz, A. Godt, G. Jeschke, A. Savitsky, M. Yulikov, EPR characterization of Mn(II) complexes for distance determination with pulsed dipolar spectroscopy, Phys. Chem. Chem. Phys. 18 (2016) 25120–25135.

[2] M. Qi, M. Hülsmann, A. Godt, Synthesis and Hydrolysis of 4-Chloro-PyMTA and 4-Iodo-PyMTA Esters and Their Oxidative Degradation with Cu(I/II) and Oxygen, Synthesis 48 (2016) 3773–3784. 3773.